

# QUALITY ASSURANCE OF PROTON BEAM PROFILE USING PHOSPHOR SCREEN AND TE-COOLED CMOS CAMERA\*

Gwangil Jung<sup>†</sup>, Young-Seok Hwang, Young Jun Yoon  
Korea Atomic Energy Research Institute, Gyeongju-si, Republic of Korea

## Abstract

The Korea Multi-Purpose Accelerator Complex (KOMAC) operates a 100 MeV proton linear accelerator, providing a high flux proton beam at the TR103, a general-purpose irradiation facility. Ensuring uniform irradiation of sample with protons is critical, necessitating confirmation of beam profile uniformity through the quality assurance (QA) process. To address this, a real-time and in-situ proton beam profile monitoring system was recently introduced and tested at the TR103. This system includes a P43 phosphor screen and TE-cooled CMOS camera, which captures images of the emitted light from protons with energies of 20, 50, and 100 MeV incident on the screen. Subsequent post-processing, such as background subtraction, image smoothing, geometrical correction, was performed on the image data. The measured beam profiles using the phosphor screen and cooled camera were then compared to those obtained using Gafchromic film<sup>TM</sup>, a widely used dosimeter in radiation measurements. Additionally, the linearity between light output and beam flux was measured to establish a quantitative relationship. This study presents the test results of the proton beam profile measurement using the phosphor screen and TE-cooled CMOS camera, demonstrating its potential as an effective tool for quality assurance in proton beam irradiation experiments at the TR103 facility.

## INTRODUCTION

Since 2013, KOMAC has operated a 100 MeV proton linear accelerator, facilitating various proton beam irradiation experiments. To ensure optimal experimental conditions and minimize irradiation errors, a rigorous quality assurance (QA) process for proton beam profiling is essential to achieve uniform proton irradiation within the sample. The uniformity criteria, defined as the difference between the maximum and minimum intensity divided by the mean intensity, must meet a threshold of 10% within the target diameter.

The TR103, a general-purpose irradiation facility at KOMAC, has used film dosimetry for beam profile QA. However, film dosimetry lacks real-time and in-situ monitoring capabilities due to the need for scanning to acquire beam profile data and its susceptibility to saturation under continuous irradiation of high-flux proton. To address these limitations, a recent advancement introduced the use of a P43 phosphor screen and TE-cooled CMOS camera for real-time and in-situ proton beam profile monitoring.

This study aimed to verify the accuracy of the P43 phosphor screen and CMOS camera system and integrated it into the quality assurance process. An experiment was conducted to capture the light response of the phosphor screen.

## EXPERIMENTS AND DISCUSSTION

### Phosphor Screen and Cooled Camera

Proton irradiation tests were performed at TR103 with a flux of approximately  $10^{10}$  to  $10^{11}$  particle/(cm<sup>2</sup>·pulse). The pulsed proton beam was accelerated to energies of 20, 45, and 102 MeV, and its energy was attenuated by 15, 42, and 100 MeV, respectively, as it passed through the beam window and air before reaching the target point. The beam profile monitoring system primarily consisted of a phosphor screen, where light is emitted as protons deposit energy, and a real-time capturing camera. The phosphor screen was positioned 1.5 m away from the beam window, tilted at a 45-degree angle relative to the beam path, while the camera was placed 1 m perpendicular to the screen for real-time imaging of the emitted light (Fig. 1).

The phosphor screen used in this study consisted of a P43 (Gd<sub>2</sub>O<sub>2</sub>S:Tb) layer on an Al substrate, providing a detection area of 310 mm × 310 mm and a peak wavelength of 545 nm [1]. With a decay time of 1 ms to 10% and high light efficiency, the phosphor screen proved suitable for real-time light emission detection. The TE-cooled CMOS camera (ASI183MC Pro, ZWO) utilized in the setup had a sensor size of 13.2 mm × 8.8 mm and a thermoelectric cooler capable of cooling sensors down to -10°C [2]. Figure 2 illustrates the arrangement of the P43 phosphor screen and the camera. To minimize image noise and avoid saturation at high light outputs, the camera

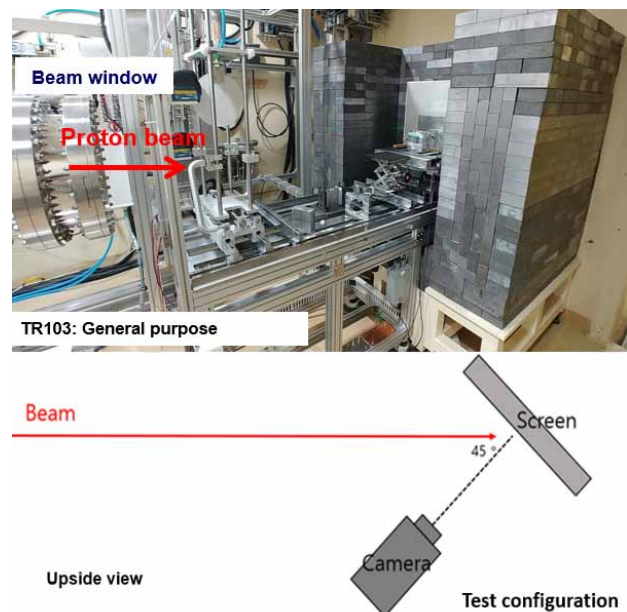


Figure 1: View of general-purpose irradiation facility, TR103 (top) and configuration of device layout (bottom).

Content from this work may be used under the terms of the CC-BY-4.0 licence (© 2023). Any distribution of this work must maintain attribution to the author(s), title of the work, publisher, and DOI

settings were optimized, utilizing the lowest ISO and appropriate exposure time.

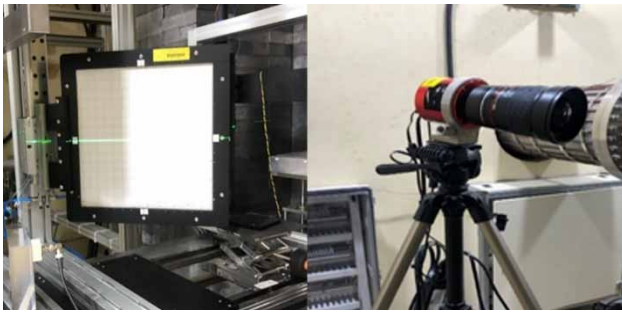


Figure 2: Setup of the P43 phosphor screen.

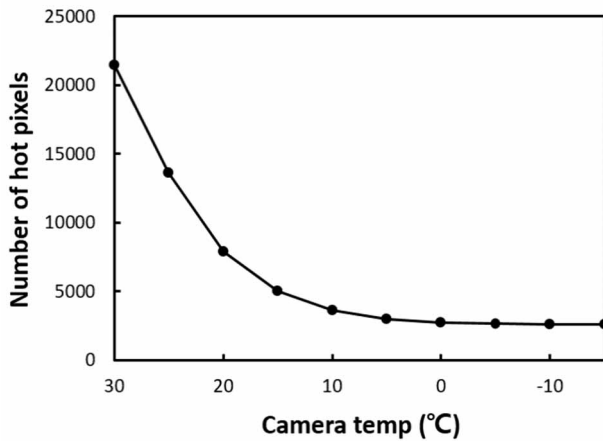


Figure 3: The number of hot pixels as a function of camera temperature.

In general, the presence of hotspots in an image is directly related to the amount of radiation accumulated in the sensor. Cooled cameras demonstrated improved radiation resistance due to the reduction of leakage current in defective sensors with decreasing temperature [3]. To validate the noise reduction effect in the high-radiation setting, an experiment was conducted to measure the number of hot pixels while cooling the pixels decreased accordingly and eventually stabilized at -10 °C, as depicted in Fig. 3.

### Image Post-Processing

To enhance the accuracy of beam profile measurements, a series of post-processing steps were employed to approximate the actual beam shape from the raw image data, as illustrated in Fig. 4. Initially, the raw image contained the white screen background and the grid, which are eliminated by subtracting pre-captured background images. Additionally, a Gaussian filter was applied to smooth the image. Considering the 45-degree tilt of the phosphor screen from the beam path, the length ratio of the horizontal axis was adjusted to reconstruct the actual beam shape. To establish X-Y coordination by converting pixels to millimetres, a Region of Interest (ROI) was selected, and the actual length of the ROI was divided by the number of pixels corresponding to that length.

An algorithm was developed to calculate the intensity uniformity within the diameter and identify the position at which the uniformity of a given diameter is minimized. A dedicated software tool was designed to facilitate the selection of beam profile image and streamline the post-processing of image data, as depicted in Fig. 5. These measures collectively contributed to increasing the accuracy and reliability of the beam profile measurements.

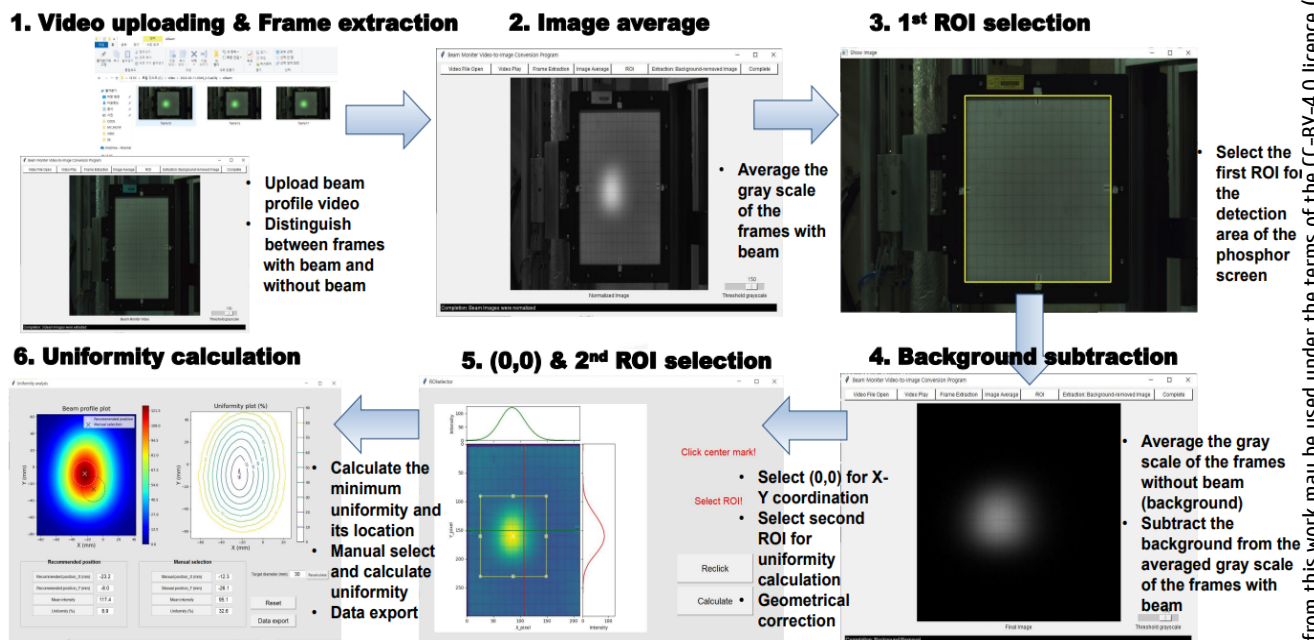


Figure 4: Post-processing of image data using Python.

Table 1: Minimum Uniformity, FWHM and Sigma of the Beam Profile Measured by Phosphor Screen and Film for Each Incident Proton Energy

	15 MeV		42 MeV		100 MeV	
	HD -V2	Screen n	HD -V2	Screen n	HD -V2	Screen n
Uniformity in 30 mm- $\phi$ (%)	11.9	9.8	7.5	7.3	6.2	6.5
Uniformity in 50 mm- $\phi$ (%)	31.1	25.6	20.2	19.8	16.1	17.1
FWHM -her (mm)	25.3	28.4	34.5	34.8	36.1	37.1
FWHM -ver (mm)	33.7	34.5	33.6	34.5	38.7	37.1
$\sigma$ -hor (mm)	21.5	24.2	29.3	29.5	30.4	31.9
$\sigma$ -ver (mm)	33.7	34.5	34.5	34.5	38.7	37.1

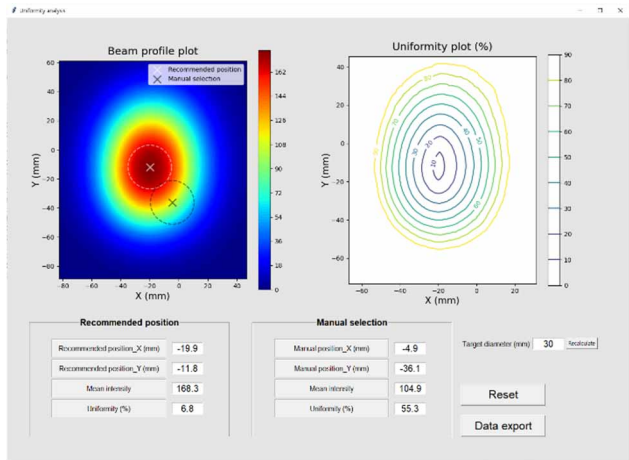


Figure 5: Uniformity calculation result window of beam profile analysis software. Software calculates the uniformity of intensity and find the position at which the uniformity of a given diameter is minimized.

### Proton Beam Profile Measurement

To compare the beam profiles obtained from the phosphor screen and film, both were subjected to 5 pulses of proton beam and subsequently normalized based on the maximum intensity value. Figure 6 presents the horizontal and vertical beam profile plots as measured by the phosphor screen. Gaussian function fitting was employed to evaluate the value of sigma and full width at half-maximum (FWHM) for the beam profile data. The minimum

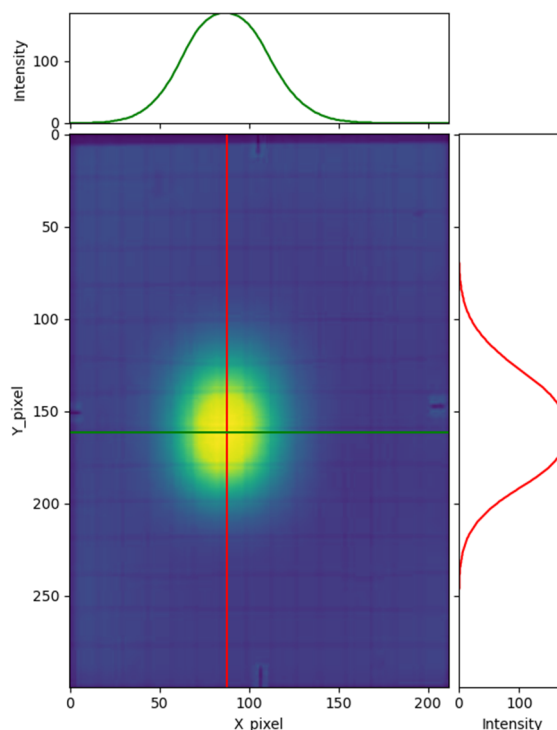


Figure 6: The horizontal and vertical beam profile plots measured by phosphor screen.

uniformity values within the Region of Interest (ROI) for diameters of 30 mm and 50 mm were calculated. Table 1 displays the minimum uniformity, FWHM, and sigma values of the beam profiles measured by the phosphor screen and film for each incident proton energy.

At incident energies of 42 MeV and 100 MeV, both the 1D profiles obtained from the phosphor screen and film display differences of less than 2 mm in both directions, while the uniformity of the 2D profile show differences within 10% for both diameters. In the case of the incident energy of 15 MeV, the 1D profile demonstrates differences of less than 3mm in both directions, and the 2D profiles exhibits differences within 20% for both diameters. These results indicate a good level of agreement and consistency between the beam profile measured using the phosphor screen and film method across various incident proton energies.

A test was conducted to verify the linearity between light output and beam flux. The faraday cup and phosphor screen were utilized simultaneously to measure beam flux and light output as the beam pulse width was increased. The beam fluxes were obtained as a function of light output for each proton energy and then normalized by the maximum value. Figure 7 illustrates the linearity between beam flux and light output for each proton energy. The corresponding R-square values for 100 MeV, 42 MeV, and 15 MeV were found to be 0.995, 0.991 and 0.961, respectively. The results demonstrated a satisfactory linearity between beam flux and light output across the entire range without any signs of saturation. However, it was observed that as the proton energy decreases, the linearity of beam flux and light output diminishes due to the influence of

Content from this work may be used under the terms of the CC-BY-4.0 licence (© 2023). Any distribution of this work must maintain attribution to the author(s), title of the work, publisher, and DOI



high linear energy transfer (LET), resulting from the low proton energy, which causes a quenching effect on light intensity [4].

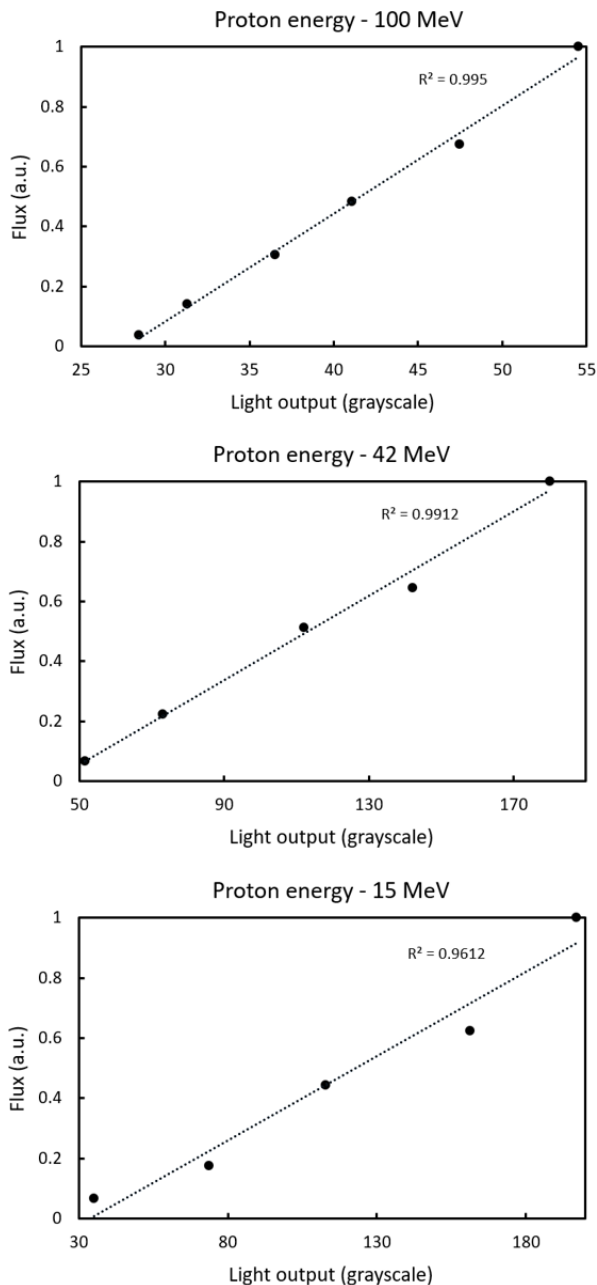


Figure 7: Beam flux as a function of light output for proton energy of 100, 42, 15 MeV.

## CONCLUSION

For real-time and in-situ proton beam profile monitoring, the integration of a P43 phosphor screen and a TE-cooled CMOS camera was implemented. To validate the accuracy of this monitoring system and incorporate it into the quality assurance process, an experiment was conducted to capture the light response of the phosphor screen using the CMOS camera. The acquired beam profile data from the phosphor screen were compared with those obtained using gafchromic film. Post-processing of the image data involved background subtraction, image smoothing, geometrical correction, and the selection of Region of Interest (ROI) and X-Y coordination.

Comparison of beam uniformity measured using the phosphor screen and film revealed that incidents with energies of 42 MeV and 100 MeV displayed differences within 10% in both diameters, while the incident energy of 15 MeV exhibited a difference of approximately 20% in both diameters. The linearity between light output and beam flux was found to be excellent, demonstrating a consistent relationship throughout the entire range without any indication of saturation.

Overall, the introduction of this novel beam profile monitoring system is expected to facilitate in-situ quality assurance processes, providing real-time monitoring capabilities and improving the accuracy and reliability of proton beam profiling at the facility.

## REFERENCES

- [1] <http://proxivision.de/product/scintillating-screen/>
- [2] <http://astronomy-imaging-camera.com/product/asi183mc-pro-color/>
- [3] A. Huber *et al.*, "Response of the imaging camera to hard radiation during JET operation", *Fusion Engineering and Design*, vol. 123, pp. 669-673, 2017.
- [4] J. B. Birks, *The Theory and Practice of Scintillation Counting*, Oxford: Pergamon, 1964.